Mode shape phase change detection in wind turbine under anisotropy variation

A. Cadoret [1,2], **E. Denimal** [2], **J.M. Leroy** [1], **J.L. Pfister** [1], **L. Mevel** [2]
[1] IFP Energies Nouvelles,
92852 Rueil-Malmaison, France
e-mail: **ambroise.cadoret@ifpen.fr**

[2] Univ. Gustave Eiffel, Inria, COSYS-SII, I4S,
35042 Rennes, France

Abstract
Fault detection by modal analysis is a highly developed field in civil engineering. For wind turbines, a loss of isotropy for the rotor can be the consequence of a defect in the angle of attack (pitch) of the blades, or the accumulation of ice, or else the presence of structural defects resulting in a loss of stiffness on one or more blades. It is highly desirable to apply classical OMA techniques, and this despite the rotation of the blades. It is shown in this paper that it is possible to apply LTI approaches on wind turbines similarly to the methodology usually applied to standard civil engineering structures using an approximate Fourier modeling of the eigenmodes. The monitoring of anisotropy using the mode shapes of the estimated modes is validated with an example where a global loss of stiffness of 5% of a rotor blade is simulated.

1 Introduction

Considering the forecasted increase in the number of wind farms in the coming years, it is important to implement reliable fault detection methods based on data collected during operation. The methods based on Operational Modal Analysis (OMA) for Linear time Invariant - modeled structures are part of the solution. The Floquet theory modeling a Linear Time Periodic system such as structures with in-operation rotating rotor is another part of the solution, provided both can be related.

To monitor a wind turbine rotor, one way is to monitor its anisotropy (or imbalance). The anisotropy can be the consequence of a pitch angle misalignment, an ice accumulation, or a structural fault. These three causes lead to different behaviors of the structure and the first two have been largely studied. Previous works have treated the stiffness anisotropy and its consequences on the dynamical behavior. The anisotropy can be seen through two indicators, namely the apparition of new harmonics in the Floquet modes in the fixed frame (nacelle and tower) and the change of amplitude and phase shift between blades in whirling modes [1]. The change of phase shift is more than 10 times more sensitive than the change of frequency [2]. The paper will be focused on the change of amplitude and phase shift.

Mainly due to the periodic behavior of an operating wind turbine (modeled as a Linear Time Periodic (LTP) system), it is theoretically not possible to use the existing OMA methods on such systems, as they no longer meet the basic OMA assumptions defined for Linear Time Invariant (LTI) systems. A first method enabling the identification of the eigenstructure of an LTP system, applied to bladed structures, is the multi-blade coordinate (MBC) method [3]. However, this method is based on the assumption of an isotropic rotor, a hypothesis that is not verified in practice. Other methods are based on the harmonic transfer function [4]. The drawback of these methods is that they require to increase the dimension of the observation space, as a consequence of the required formalism. Another problem is that these methods require knowledge of the actual rotational speed of the system. A last group of methods is those adapting the classical subspace methods. One example is the SSI LPTV method [5], which allows to correctly identify the exact eigenmodes

of an LTP system, the so-called Floquet modes. However, this method converges in period number, which is more suitable for systems with a high rotational speed such as helicopters. To overcome the difficulty to define an identification method for LTP systems, an approach based on the approximation of the LTP eigenmodes defined in [6] is used. This approximation leads to the definition of modes similar to the LTI modes, that can be identified with the existing OMA methods.

The identification of structural modes with OMA is a stochastic procedure, so identified modes are uncertain. Therefore, to decide if the structure has changed, it is needed to obtain the identified modes coupled with their uncertainties. With the existing OMA methods such as the Stochastic Subspace Identification (SSI) [7], it is possible to use an uncertainty computation method [8], based on the first order delta method. As the objective is to monitor the phase shift and the amplitude, the uncertainty of both quantities needs to be developed.

In this paper, a method to detect anisotropy based on the study of the evolution of the phase shift and the amplitude using the blade root moments is proposed. The mode shapes of the reference structure (considered healthy) are compared to the current (considered to be possibly damaged) identified eigenmodes by studying phases and amplitudes change while including the associated uncertainties. Finally, the eigenmodes are also compared with the Modal Assurance Criterion (MAC) and its associated uncertainty computation [9] to validate the anisotropy detection method and thus demonstrate its effectiveness for wind turbine monitoring.

The organisation of the paper is as follows. Section 2 presents the proposed approach for performing OMA on operating wind turbines. Section 3 assesses the impact of the rotor anisotropy on the eigenmodes. Then, Section 4 introduces the considered underlying identification method and defines the associated uncertainty quantification. Finally, Section 5 shows that phase shift and amplitude can be used for fault detection, with an application of the defined damage detection method on simulated data.

2 OMA approach for wind turbines

2.1 Dynamic model

The motion of a constant rotating wind turbine can be expressed as an LTP-system,

$$\mathcal{M}(t)\ddot{\xi}(t) + \mathcal{C}(t)\dot{\xi}(t) + \mathcal{K}(t)\xi(t) = v(t), \tag{1}$$

where $\xi(t) \in \mathbb{R}^m$ represents the displacements of the structure at the degrees of freedom (DOF) of the system, and $\mathcal{M}(t+T) = \mathcal{M}(t)$, $\mathcal{C}(t+T) = \mathcal{C}(t)$, $\mathcal{K}(t+T) = \mathcal{K}(t)$, respectively the mass, damping and stiffness matrices. T represents the rotational period. The unknown input $v(t)$ is assumed to be a Gaussian white noise. In the following, the mechanical system is expressed in a state-space form, from the definition of the state vector $x(t) \in \mathbb{R}^n$ where $n = 2m$ and the observation $y(t) \in \mathbb{R}^r$.

$$x(t) = \begin{bmatrix} \xi(t) \\ \dot{\xi}(t \end{bmatrix} \quad \text{and} \quad y(t) = C_a\ddot{\xi}(t) + C_v\dot{\xi}(t) + C_d\xi(t), \tag{2}$$

where C_a, C_v and C_d are selection matrices. A noise $w(t)$ can be added to the observation. $w(t)$ is assumed to be a Gaussian white noise. This leads to the following state-space expression:

$$\begin{cases} \dot{x}(t) = A_c(t)x(t) + B_c(t)v(t) \\ y(t) = C(t)x(t) + D(t)v(t) + w(t) \end{cases}, \tag{3}$$

with all the matrices defined in [6]. Using the Floquet theory [10, 11], the homogeneous part of the state vector can be expressed as a sum of n eigenmodes with a periodic amplitude, namely the Floquet modes

$$x_h(t) = \sum_{j=1}^{n} X_j(t) \exp(\mu_j t)\, q_j(t_0), \tag{4}$$

with μ_j the j–th characteristic exponent, $q_j(t_0)$ depending of the initial conditions and $X_j(t)$ the associated T-periodic amplitude.

2.2 Approximation of the Floquet modes

Once the Floquet mode decomposition is applied, the observation vector is expressed as a finite sum of eigenmodes to obtain the description of a time invariant system. Similarly, the Floquet mode decomposition of the observation $y_h(t)$ is

$$y_h(t) = \sum_{j=1}^{n} Y_j(t) \exp(\mu_j t)\, q_j(t_0), \tag{5}$$

where $Y_j(t) = C(t)X_j(t)$ is both the amplitude of the j–th Floquet mode of the observation and a periodic vector of period $T = \frac{2\pi}{\Omega}$. Using Equation (5) and expanding into a Fourier series the amplitudes of the Floquet modes, it comes

$$y_h(t) = \sum_{j=1}^{n} \sum_{l=-\infty}^{\infty} Y_{j,l} \exp((\mu_j + il\Omega)\, t)\, q_j(t_0). \tag{6}$$

with $Y_{j,l}$ the Fourier coefficients. The contributions of the harmonics in the expansion of $y_h(t)$ are determined by the participation factor [12]

$$\phi^y_{j,l} = \frac{\|Y_{j,l}\|}{\sum_{l=-\infty}^{\infty} \|Y_{j,l}\|}. \tag{7}$$

A minimum participation factor (ϕ^y_{min}) is applied to select harmonics with the highest contribution. Then, an approximation of the observation is constructed as $\hat{y}(t)$ by a finite sum of eigenmodes,

$$\hat{y}_h(t) = \sum_{(j,l),\phi^y_{j,l} \geq \phi^y_{min}} Y_{j,l} \exp((\mu_j + il\Omega)\, t)\, q_j(t_0), \tag{8}$$

$\hat{y}(t)$ can then be expressed as a sum of $\tilde{n}$ eigenmodes

$$\hat{y}_h(t) = \sum_{p=1}^{\tilde{n}} Y_p \exp(\mu_p t)\, q_p(t_0), \tag{9}$$

where each index p corresponds to a pair (j, l) and $\mu_p = \mu_j + il\Omega$.

Finally the Floquet modes of an LTP-system have been approximated by a finite number of eigenmodes identical to those of an LTI-system. Consequently the dynamical behavior of an LTP-system can theoretically be approximated as the behavior of an LTI-system. This approximation has been demonstrated in [6] and used with a subspace identification of a multi-physics model of wind turbine model in [13]. In the next section, the evolution of the approximation eigenmodes regarding the rotor anisotropy is assessed, with an application to the DTU 10MW model of wind turbine [14].

3 Impact of the anisotropy on the eigenmodes

To assess a change in the approximation eigenmodes, the approximation of the DTU 10MW wind turbine model is computed for three different stiffness reductions for one blade, namely 1%, 2.5% and 5%. With the software OpenFAST [15], the system matrices are linearized and used to integrate the homogeneous equation. The approximation can then be computed using the formalism defined in Section 2.

In this paper, the vocabulary commonly used in wind energy is used. Side-Side and Fore-Aft denote the tower bending respectively in and out of the rotor plane. Edge and Flap denote the blades bending respectively in and out of the rotor plane. For the edge bending, different modes have to be considered, the Collective edge represents the in-phase bending of the blades. Backward and Forward Edge correspond to out of phase

bending of the blades, for the Backward edge the bending of the second blade is delayed compared to the first blade. For the Forward edge, the bending of the second blade is in advance compared to the bending of the first blade. These two bending modes have an impact on the tower dynamical properties, with respectively a frequency of $f_{bw} - \frac{\Omega}{2\pi}$ and $f_{fw} + \frac{\Omega}{2\pi}$, where Ω denotes the rotational speed of the rotor.

First, the change in the eigenfrequency can be assessed. In Table 1, the evolution of the natural frequencies of some approximation modes is summarised depending on the increase of the stiffness loss for the damaged blade. It has been computed for a rotational speed of 6 rpm. Looking at the results, one can see that whatever the loss in stiffness is for the damaged blade, the frequency change remains negligible. Indeed, the difference between the natural frequencies between the two structural states is negligible, with a maximum of 0.015 Hz for the collective edge. This order of magnitude is not significant for a real structure, where the effects of varying environmental conditions will be more important. Consequently, the frequency cannot be used a reliable indicator to detect changes in the rotor properties. So, another approach is investigated and the change in the mode shapes due to the anisotropy will be assessed, as it is introduced in [2, 1].

Table 1: Some frequencies of the LTI approximation in function of the stiffness for the third blade

Name	Isotropic	99% of stiff.	97,5% of stiff.	95% of stiff.
2-SS	2.349	2.348	2.348	2.348
Col. Edge	2.061	2.058	2.054	2.046
Fw. Tower	1.108	1.107	1.106	1.105
Fw. Rotor	1.008	1.007	1.006	1.005
Bck. Rotor	1.001	0.999	0.995	0.988
Bck. Tower	0.901	0.899	0.896	0.888
1-FA	0.257	0.257	0.257	0.257
1-SS	0.253	0.253	0.253	0.253

Figure 1 represents the evolution of the amplitude and the phase shift between the blades on a polar plot for the different considered stiffness reductions, where each subfigure corresponds to a different mode. First, it has to be noted that the first blade defines the reference, with an amplitude equal to 1 and a phase to 0. The choice of the reference blade will have an impact on the values of phase shift and amplitude, but the global change compared to the isotropic state will be the same. Figures 1b and 1c show that there is an important evolution of the phase shift for the backward and forward edge bending modes coupled with an important evolution of their amplitude. Indeed, for the isotropic state, the phase shift between each blade is 120° and the amplitude is equal to 1 for each blade. For a stiffness loss of 5%, the phase shift decreases to about 50° and 190° for the 2nd and 3rd blades for the backward edge bending mode respectively, whereas the vibration amplitude decreases for the 2nd blade and increases for the third one. Considering the forward edge bending mode, the amplitudes for both blades decrease but it decreases substantially for the 2nd blade (to about 0.2). The phase shift of the second blade remains somewhat constant and equal to 120°, whereas it decreases for the third blade. The collective edge has a different evolution compared to the two others. Indeed, only the amplitude of the damaged blade is evolving with a reduction of the amplitude in function of the loss of stiffness. These results illustrate the high sensitivity of the phase shift and the amplitude to anisotropy and the relevance of tracking these parameters to monitor a wind turbine.

Table 2: MAC criterion of the whirling mode, computed between the isotropic and the anisotropic modes for different anisotropy levels

Mode	Stiff. 99%	Stiff. 97.5%	Stiff. 95%
Col.	0.999	0.996	0.982
Bck.	0.968	0.846	0.691
Fw.	0.973	0.849	0.704

Table 2 summarizes the MAC between the mode shapes of the isotropic state and the anisotropic states. It confirms the graphical analysis as a larger evolution of the MAC is observed for the backward and forward

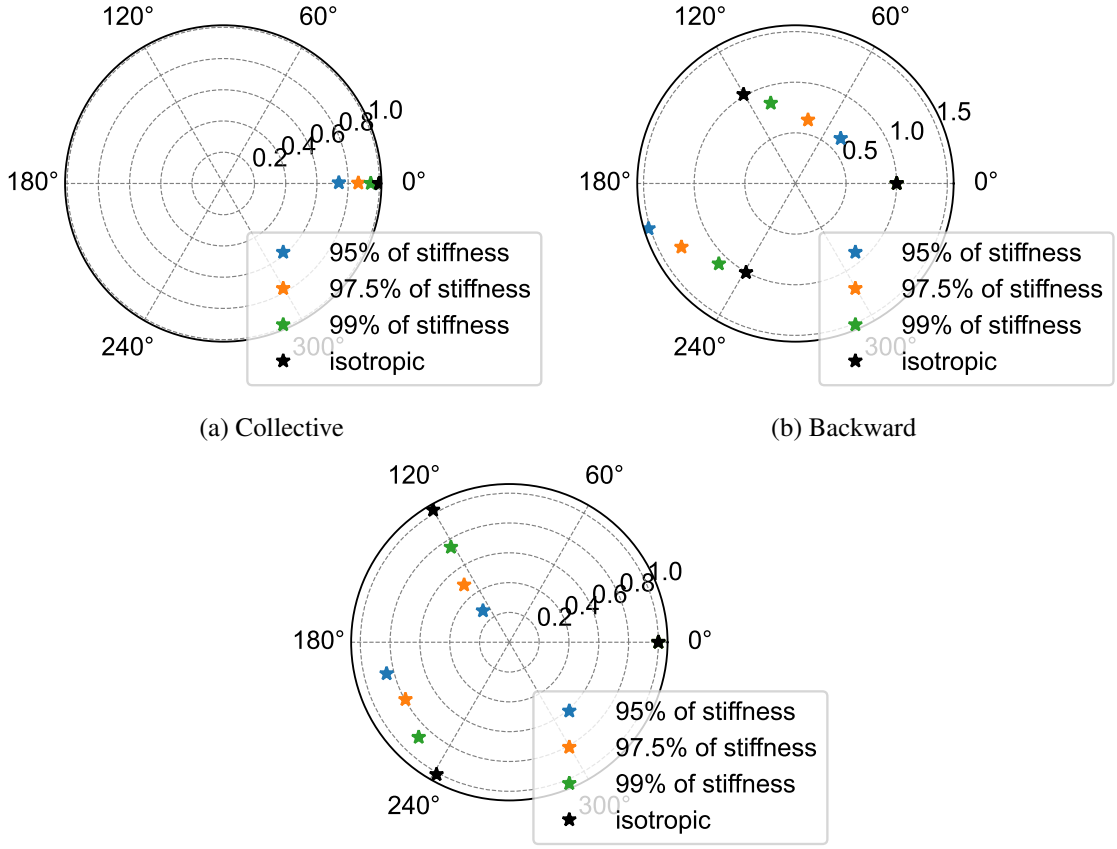

(a) Collective

(b) Backward

(c) Forward

Figure 1: Evolution of the polar plot of the edgewise bending mode shapes against the third blade stiffness

edge mode shapes. It can be concluded that the mode shapes of the backward and the forward edge have a similar sensitivity to the anisotropy. The mode shape of the collective edge is less affected globally by the change scenarios since only the amplitude of the damaged blade is affected by the rotor anisotropy.

As a conclusion, due to the important sensitivity of the mode shapes of the edge bending modes regarding the anisotropy, the mode shapes can be used to detect the anisotropy. The next section is dedicated to the introduction of a subspace identification method and the definition of the uncertainties of the amplitude and the phase shift.

4 Identification method and uncertainty computation

4.1 Stochastic Subspace Identification (SSI)

Before performing the subspace identification, the state-space representation of the approximation is needed. From the definition of an LTP-system and its associated approximation, it is possible to define the following discrete state-space

$$\begin{cases} z_{k+1} = \mathbf{A} z_k + \mathbf{B}_k v_k \\ y_k = \mathbf{C} z_k + \mathbf{D}_k v_k + \tilde{w}_k \end{cases}, \tag{10}$$

with z_k the new state vector based on the approximation of the outputs, $\mathbf{A}$ and $\mathbf{C}$ two constant matrices and $\mathbf{B}_k$ and $\mathbf{D}_k$ two periodic matrices of period $T_d = \frac{T}{\Delta t}$ (Δt the data time step). The complete definition of the state-space of the approximation and the demonstration of the applicability of the Stochastic Subspace Identification (SSI) method is detailed in [6]. Here, an efficient version [16] of the SSI method [7] is used. The

SSI [7] aims to identify the eigenmodes of the system through the sample correlations. The SSI covariance-driven is presented in the following. The first step is to construct a Hankel matrix filled by correlations, directly constructed from matrices gathering the observation data

$$\hat{H} = \mathcal{Y}^{+} \left(\mathcal{Y}^{-}\right)^{T}. \tag{11}$$

where $\mathcal{Y}^{+} \in \mathbb{R}^{(p+1)r \times N}$ and $\mathcal{Y}^{-} \in \mathbb{R}^{qr \times N}$ are defined in [7]. $\hat{H}$ can be seen as the Hankel matrix filled with the correlations $\hat{R}_i$, the estimate of the correlation $R_i = \mathbb{E}\left(y_k y_{k-i}^T\right) = \mathbf{C}\mathbf{A}^{i-1}G$, where $G = \mathbb{E}\left(z_{k+1} y_k^T\right)$. From the estimation of the Hankel matrix, by using a singular value decomposition it is possible to identify the system matrices **A** and **C**. Then, the eigenmodes can be computed with the eigenvalue decomposition of **A**

$$\mathbf{A} = \Psi \left[\mu_i\right] \Psi^{-1}. \tag{12}$$

The continuous time eigenvalues λ_i are found from the discrete time eigenvalues μ_i by $\lambda_i = \frac{\log(\mu_i)}{\Delta t}$. Then the frequency ($f_i$) and the damping ($\zeta_i$) of the associated mode are defined such that $f_i = \frac{|\lambda_i|}{2\pi}$ and $\zeta_i = -100.\frac{Re(\lambda_i)}{|\lambda_i|}$. Finally, the mode shape matrix is found from $\Phi = \mathbf{C}\Psi$.

4.2 Uncertainty computation

Following the identification, an uncertainty computation method is used [17]. Defined in [8], the method estimates the covariance matrices of the identified modes from the same data used for the identification. From the covariance matrices, it is possible to express the standard deviations σ_f and σ_ζ of the frequency and damping, respectively.

To perform the uncertainty quantification, the delta method and a first order approximation are used. Thus, using the sensitivity matrix of the considering parameter regarding the correlations and the covariance matrices of correlations ($\hat{\Sigma}_R$), the covariance matrix of all the identified parameters can be computed. For example, the covariance matrix of an eigenfrequency is

$$\hat{\text{cov}}(f_i) = \mathcal{J}_{f_i} \hat{\Sigma}_R \mathcal{J}_{f_i}^T. \tag{13}$$

Where $\mathcal{J}_{f_i}$ denotes the sensitivity of the i–th eigenfrequency regarding the correlations, with $\mathcal{J}_{f_i} = \frac{\partial f_i}{\partial vec(R)}$. The sensitivity of the frequencies, damping and mode shapes of the eigenmodes are defined in [17].

In the previous section, it has been shown that the phase shift and the amplitude are good indicators of the rotor anisotropy. Consequently, the sensitivity of the phase shift and the amplitude will be defined in the next section.

4.3 Definition: Sensitivity of phase shift and amplitude

First, let us define the phase shift P_j of a mode shape $\phi \in \mathbb{R}^r$ at the degree of freedom j. The mode shape at the DOF j can be defined as

$$\begin{aligned} \phi_j &= a_j \exp\left(iP_j\right) \\ &= a_j \cos\left(P_j\right) + i a_j \sin\left(P_j\right), \end{aligned}$$

where a_j denotes the amplitude. From this expression, the phase shift can be defined as

$$P_j = \arctan\left(\frac{\Im(\phi_j)}{\Re(\phi_j)}\right). \tag{14}$$

As it was introduced in the previous section, to estimate the uncertainty of a quantity, its sensitivity from another quantity has to be defined. So, the sensitivity of the phase shift regarding the mode shape is defined

as

$$\mathcal{J}_{P,\phi} = \left[\frac{\partial P}{\partial \Re(\phi)} \quad \frac{\partial P}{\partial \Im(\phi)}\right] \in \mathbb{R}^{r\times 2r}. \tag{15}$$

First

$$\frac{\partial P_j}{\partial \Re(\phi_j)} = -\frac{\Im(\phi_j)}{\Re(\phi_j)^2}\frac{1}{1+\left(\frac{\Im(\phi_j)}{\Re(\phi_j)}\right)^2} \tag{16}$$

$$= \frac{-\Im(\phi_j)}{|\phi_j|^2}, \tag{17}$$

analogously

$$\frac{\partial P_j}{\partial \Im(\phi_j)} = \frac{1}{\Re(\phi_j)}\frac{1}{1+\left(\frac{\Im(\phi_j)}{\Re(\phi_j)}\right)^2} \tag{18}$$

$$= \frac{\Re(\phi_j)}{|\phi_j|^2}. \tag{19}$$

Finally, the definition of $\mathcal{J}_{P,\phi}$ is

$$\mathcal{J}_{P,\phi} = \left[\left[\frac{-\Im(\phi_k)}{|\phi_k|^2}\right] \quad \left[\frac{\Re(\phi_k)}{|\phi_k|^2}\right]\right], \tag{20}$$

with $\left[\frac{\Im(-\phi_k)}{|\phi_k|^2}\right] \in \mathbb{R}^{r\times r}$ a diagonal matrix, as for $\left[\frac{\Re(\phi_k)}{|\phi_k|^2}\right]$.

$\mathcal{J}_{P,\phi}$ is defined and non-zero if ϕ is non-zero for all degrees of freedom. This condition is verified if the associated mode shape is non zero at every sensor. If a mode shape has a zero amplitude at a sensor, it is not useful to compute the phase shift and its uncertainty.

The amplitude (a_i) of the DOF i of the mode shape ϕ is defined as

$$a_i = |\phi_i| = \sqrt{\Re(\phi_i)^2 + \Im(\phi_i)^2}. \tag{21}$$

Analogously as previously, the sensitivity of the amplitude regarding the mode shape has to be defined,

$$\mathcal{J}_{a,\phi} = \left[\frac{\partial a}{\partial \Re(\phi)} \quad \frac{\partial a}{\partial \Im(\phi)}\right] \in \mathbb{R}^{r\times 2r}. \tag{22}$$

First

$$\frac{\partial a_i}{\partial \Re(\phi_i)} = \frac{\Re(\phi_i)}{|\phi_i|}, \tag{23}$$

and

$$\frac{\partial a_i}{\partial \Im(\phi_i)} = \frac{\Im(\phi_i)}{|\phi_i|}. \tag{24}$$

Finally, the sensitivity matrix ($\mathcal{J}_{a,\phi}$) is defined as

$$\mathcal{J}_{a,\phi} = \left[\left[\frac{\Re(\phi_k)}{|\phi_k|}\right] \quad \left[\frac{\Im(\phi_k)}{|\phi_k|}\right]\right], \tag{25}$$

with $\left[\frac{\Re(\phi_k)}{|\phi_k|}\right] \in \mathbb{R}^{r\times r}$ a diagonal matrix, as for $\left[\frac{\Im(\phi_k)}{|\phi_k|}\right]$. Like $\mathcal{J}_{P,\phi}$, $\mathcal{J}_{a,\phi}$ is defined and non-zero if ϕ is non-zero for all sensors.

An identification method and the associated uncertainties have been defined, now this method will be used to monitor the change of the identified edgewise bending mode shapes with the analysis of the phase shift and the amplitude, to detect anisotropy.

5 Anisotropy detection method

5.1 Method to detect rotor anisotropy

As the identified modes are obtained from correlation estimates, they are uncertain. Thus, to determine if a mode shape has changed it is necessary to compare the identified values with the associated uncertainties. The Modal Assurance Criterion (MAC) [18] can be used to asses the difference between two mode shapes (ϕ, ψ)

$$MAC(\phi, \psi) = \frac{\left|\phi^H \psi\right|^2}{\left(\phi^H \phi\right)\left(\psi^H \psi\right)}. \tag{26}$$

Also this criterion can be used to determine if two mode shapes are statistically distinct. In [9] it has been shown that the MAC follows different statistical laws depending on the compared mode shapes. If the compared mode shapes are identical, the criterion follows a χ^2 law and if the mode shapes are different, it follows a Gaussian law. For the χ^2 law, the confidence interval is defined with the lower bound of the 95% quantile as the upper bound is 1. For the Gaussian law, the confidence interval is computed with the standard deviation.

The objective of the method is to asses changes in the mode shapes. To achieve such goal, an actual set of identified eigenmodes has to be compared to a reference set. Precisely, a change in rotor isotropy is sought through changes in the edgewise bending modes. The method to detect anisotropy changes is composed of the following steps:

1. Identification of the reference state using only the blade root edge-moment: uncertainty computation of the mode shape, amplitude and phase shift
2. Identification of the actual state (potentially damaged) using only the blade root edge-moment: uncertainty computation of the mode shape, amplitude and phase shift
3. Comparison of the mode shape of edgewise bending and their associated uncertainties on a polar plot. The compared estimated mode shapes are not corresponding to the same state if the 95% confidence intervals do not cross each other
4. Computation of the MAC criterion and the associated uncertainties. If the MAC follows a χ^2 law the mode shapes are considered to be corresponding to the same state, and if the MAC follows a Gaussian law the mode shapes are corresponding to different states and anisotropy is detected

Now this method will be tested, with an change scenario in the DTU 10MW rotor isotropy.

5.2 Detection of 5% loss of stiffness under turbulent wind

In this example, a loss of 5% of stiffness on the third blade is simulated for the damaged state. To have the same environmental conditions, both states (reference and damaged) are simulated with the same turbulent wind. The wind speed and the rotational speed are illustrated in Figure 2a.

With Figures 2b, 2c and 2d, the mode shapes of the three edge bending modes can be compared. These figures represent the phase shift and the amplitudes of the three blades with their uncertainty intervals for the three different modes considered. As it was stated in Section 3, the first blade defines the reference, so the associated phase and amplitude to this blade are exact (without uncertainty). In Figures 2b and 2d, the confidence intervals of the reference and damaged state do not cross each other. It can be concluded, that the associated mode shapes are different for the Backward and Collective edge. In Figure 2c, the confidence intervals are crossing each other, so the corresponding mode shapes can not be considered to be different. Now, this graphical analysis will be validated, with the study of the statistical law of the MAC.

Table 3 summarizes the MAC and uncertainties of each mode. For the Collective and Backward edge, the value of the identified MAC is below the lower bounds of the 95% quantile defined with a chi-square law

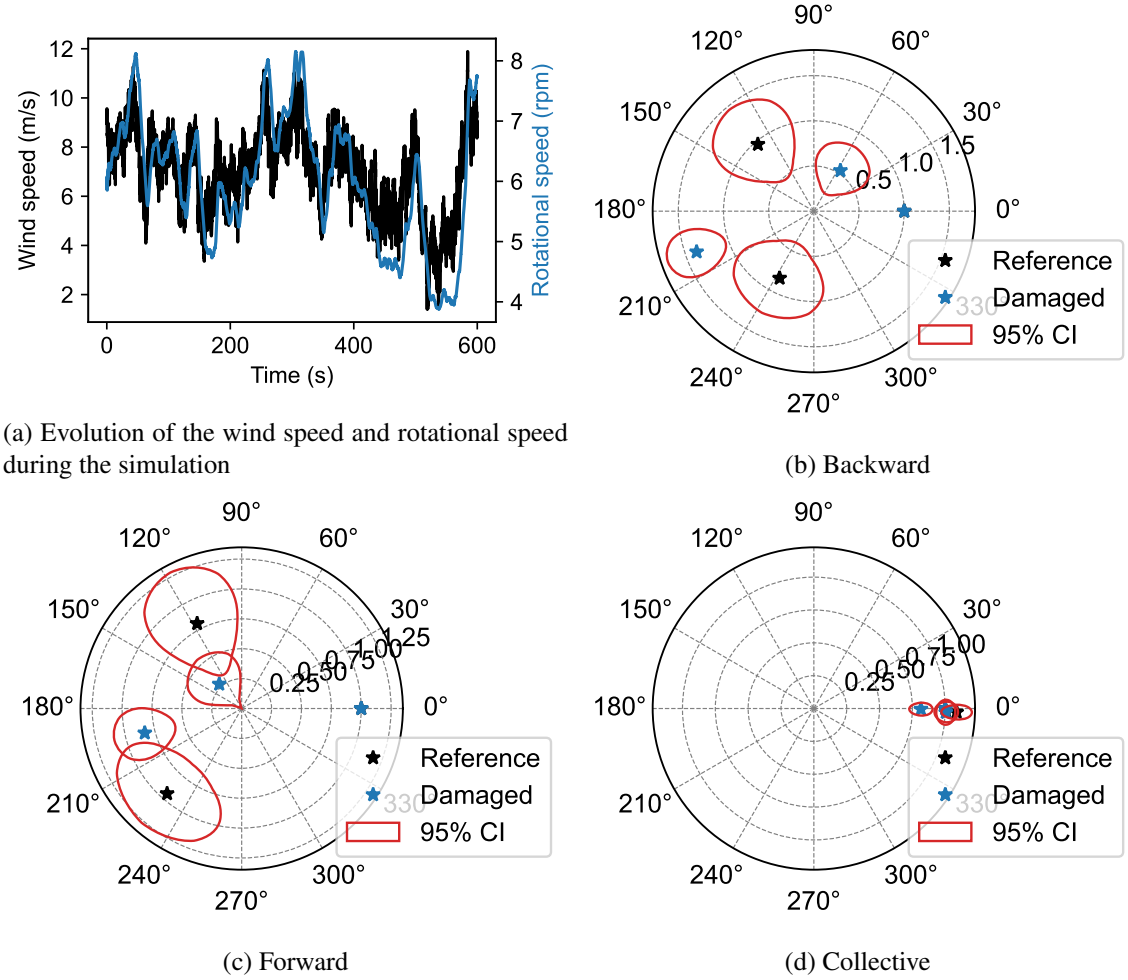

(a) Evolution of the wind speed and rotational speed during the simulation

(b) Backward

(c) Forward

(d) Collective

Figure 2: Comparison of the edgewise bending mode shapes between the reference state and the damaged state under a turbulent wind

modelling. This confirms that the mode shapes of the damaged state are different from those of the reference state. Also, the MAC of the Forward edge mode seems to follow a chi-square law, meaning that the mode shapes are close or similar. Consequently, the uncertainty analysis for the MAC is validating the graphical analysis based on the confidence interval.

6 Conclusion

It has been shown that the amplitude and phase of the mode shape of the edge bending modes are good indicators of the rotor anisotropy. So, a method to monitor the change of those quantities has been defined. Regarding the results, it can be concluded that the analysis of the edgewise bending mode shapes can be used to detect fault corresponding to a loss of 5% of stiffness on one blade. It is possible to use the amplitudes of

Table 3: MAC criterion and the respective uncertainties, under a turbulent wind

Name	MAC	Standard deviation	Quantile
Col.	0.9827	0.0089	0.9913
Bck.	0.6672	0.1565	0.7853
Fw.	0.8063	0.1515	0.6846

the collective mode shape for the fault localization.

Future works, will be dedicated to automation of the fault detection method and development of more sophisticated methods using the evolution of the phase shift and amplitude.

References

[1] D. Tcherniak, "Rotor anisotropy as a blade damage indicator for wind turbine structural health monitoring systems," *Mechanical Systems and Signal Processing*, vol. 74, pp. 183–198, 2016.

[2] E. Di Lorenzo, "Operational modal analysis for rotating machines," Ph.D. dissertation, University of Naples" Federico II, 2017.

[3] G. Bir, "Multi-blade coordinate transformation and its application to wind turbine analysis," in *46th AIAA Aerospace Sciences Meeting and Exhibit*. [Reston, VA]: [American Institute of Aeronautics and Astronautics], 2008.

[4] M. S. Allen, M. W. Sracic, S. Chauhan, and M. H. Hansen, "Output-only modal analysis of linear time-periodic systems with application to wind turbine simulation data," *Mechanical Systems and Signal Processing*, vol. 25, no. 4, pp. 1174–1191, 2011.

[5] A. Jhinaoui, L. Mevel, and J. Morlier, "A new ssi algorithm for lptv systems: Application to a hinged-bladed helicopter," *Mechanical Systems and Signal Processing*, vol. 42, no. 1-2, pp. 152–166, 2014.

[6] A. Cadoret, E. Denimal, J.-M. Leroy, J.-L. Pfister, and L. Mevel, "Linear time invariant approximation for subspace identification of linear periodic systems applied to wind turbines," in *11th IFAC Symposium on Fault Detection, Supervision and Safety for Technical Processes - SAFEPROCESS*, Pafos, Cyprus, 2022.

[7] P. van Overschee and B. de Moor, "Subspace algorithms for the stochastic identification problem," *Automatica*, vol. 29, no. 3, pp. 649–660, 1993.

[8] E. Reynders, R. Pintelon, and G. de ROECK, "Uncertainty bounds on modal parameters obtained from stochastic subspace identification," *Mechanical Systems and Signal Processing*, vol. 22, no. 4, pp. 948–969, 2008.

[9] S. Greś, M. Döhler, and L. Mevel, "Uncertainty quantification of the modal assurance criterion in operational modal analysis," *Mechanical Systems and Signal Processing*, vol. 152, p. 107457, 2021.

[10] G. Floquet, "Sur la théorie des équations différentielles linéaires," in *Annales Scientifiques de L'École Normale Supérieure*, vol. 8, 1879, pp. 3–132.

[11] P. F. Skjoldan and M. H. Hansen, "On the similarity of the coleman and lyapunov–floquet transformations for modal analysis of bladed rotor structures," *Journal of Sound and Vibration*, vol. 327, no. 3, pp. 424–439, 2009.

[12] C. L. Bottasso and S. Cacciola, "Model-independent periodic stability analysis of wind turbines," *Wind Energy*, vol. 18, no. 5, pp. 865–887, 2015.

[13] A. Cadoret, E. Denimal, J.-M. Leroy, J.-L. Pfister, and L. Mevel, "Periodic system approximation for operational modal analysis of operating wind turbine," in *EWSHM 2022 - 10th Workshop on Structural Health Monitoring*, Palermo, Italy, 2022.

[14] DTU, "dtu-10mw-rwt," https://rwt.windenergy.dtu.dk/dtu10mw/dtu-10mw-rwt, accessed: 2021-06-03.

[15] NREL, "Openfast v2.5.0," https://github.com/OpenFAST/openfast/releases/tag/v2.5.0, accessed: 2021-06-03.

[16] M. Döhler and L. Mevel, "Fast multi-order computation of system matrices in subspace-based system identification," *Control Engineering Practice*, vol. 20, no. 9, pp. 882–894, 2012.

[17] M. Döhler and L. Mevel, "Efficient multi-order uncertainty computation for stochastic subspace identification," *Mechanical Systems and Signal Processing*, vol. 38, no. 2, pp. 346–366, 2013.

[18] M. Pastor, M. Binda, and T. Harčarik, "Modal assurance criterion," *Procedia Engineering*, vol. 48, pp. 543–548, 2012.